Rapid Communications

Enhanced Seebeck coefficient by a filling-induced Lifshitz transition in K_xRhO_2

Naoko Ito,* Mayu Ishii, and Ryuji Okazaki†
Department of Physics, Faculty of Science and Technology, Tokyo University of Science, Noda 278-8510, Japan

(Received 7 November 2018; published 16 January 2019)

We have systematically measured the transport properties in the layered rhodium oxide K_xRhO_2 single crystals ($0.5 \lesssim x \lesssim 0.67$), which is isostructural to the thermoelectric oxide Na_xCoO_2. We find that below $x = 0.64$ the Seebeck coefficient is anomalously enhanced at low temperatures with increasing x, while it is proportional to the temperature as a conventional metal above $x = 0.65$, suggesting the existence of a critical content $x^* \simeq 0.65$. For the origin of this anomalous behavior, we discuss a filling-induced Lifshitz transition, which is characterized by a sudden topological change in the cylindrical hole Fermi surfaces at the critical content x^*.

DOI: 10.1103/PhysRevB.99.041112

The layered cobalt oxide Na_xCoO_2 has attracted a great deal of attention for its rich physical properties since the discovery of the large Seebeck coefficient [1]. This compound consists of alternately stacked CoO_2 and Na layers, and the conductive CoO_2 layer is formed by edge-shared CoO_6 octahedra, resulting in a two-dimensional (2D) triangular lattice of Co ions. The uniqueness of this compound is the complex electronic properties drastically changing with Na content x [2]. For a rich Na content region, the large Seebeck coefficient is observed with metallic resistivity [3,4]. The magnetic property varies from Pauli-paramagnetic to Curie-Weiss (CW) behavior across a critical Na content $x^*_{Na} \simeq 0.62$ [5–8]. A spin-density-wave and a charge-ordered insulating state have also been suggested for $0.75 \leqslant x$ and at $x \sim 0.5$, respectively [9–13]. Moreover, hydration induces unconventional superconductivity at around $x = 0.3$ [14–18].

The crucial points for understanding various emergent phenomena in Na_xCoO_2 are the characteristic electronic band structure and the topology of the Fermi surface. In this compound, the t_{2g} bands from Co $3d$ orbitals are composed of an a_{1g} band and doubly degenerate e'_g bands, and the Fermi level lies across the a_{1g} band to form a cylindrical Fermi surface reflecting the quasi-2D crystal structure [19–27]. Now the shape of the a_{1g} band is peculiar, including a somewhat flat portion around a local minimum at the Γ point, which is called a pudding-mold band shape [28]. With increasing Na content, the Fermi level rises and then touches the local minimum to create a small electron pocket as is resolved by angle-resolved photoemission spectroscopy (ARPES) [27]. A detailed thermodynamic study has revealed that this topological change in the Fermi surface, known as the Lifshitz transition [29], occurs at the critical content $x^*_{Na} \simeq 0.62$ [8]. The Fermi level then locates around the flat region for $x > x^*_{Na}$, resulting in a large Seebeck coefficient due to a significant difference in the velocities of electrons and holes [28]. The flat band with a large density of states may also contribute to the CW-like magnetic behavior observed above x^*_{Na}.

The issue to be addressed is whether the richness of these intriguing properties universally emerges in the related systems. K_xCoO_2 ($x \sim 0.5$) shows two phase transitions at low temperatures [30,31], reminiscent of $Na_{0.5}CoO_2$, and similar electronic structures in these materials are suggested both experimentally and theoretically [25,32]. The $4d$ system Na_xRhO_2 is also isostructural to Na_xCoO_2 [33,34] and exhibits a metal-insulator transition which is explained by an Ioffe-Regel criterion [35], but the detailed electronic properties are still unexplored.

The isostructural K_xRhO_2 shows a moderately large Seebeck coefficient with half the magnitude of Na_xCoO_2 [36–38]. An optical study suggests that the bandwidth of K_xRhO_2 is twice broader compared with Na_xCoO_2 owing to a difference of the orbital sizes between Co $3d$ and Rh $4d$ electrons [39]. A recent ARPES measurement has clarified that the band shape of K_xRhO_2 is closely similar to that of Na_xCoO_2 [40], indicating a possible emergence of a rich electronic phase diagram. Furthermore, interesting phenomena, including a significant enhancement of thermoelectric efficiency by hydration [41] and a realization of a topological quantum Hall effect [42], have been theoretically predicted in K_xRhO_2. However, the physical properties of K_xRhO_2 are little known due to the difficulty of the synthesis of well-controlled K content, single-phase samples [43,44].

In this Rapid Communication, we present the potassium composition dependence of the transport properties in K_xRhO_2 for $0.5 \lesssim x \lesssim 0.67$ using pure single-crystalline samples, which are systematically prepared by a self-flux method and a K deintercalation process. We find that the Seebeck coefficient is highly sensitive to the K content x and enhanced only below a critical content $x^* \simeq 0.65$. This result is attributed to a filling-induced Lifshitz transition at x^*, at which the topology of the cylindrical hole surface dramatically changes. Moreover, near $x = 0.5$, a distinct anomaly is observed at $T \simeq 75$ K, implying that this rhodate also offers a fascinating platform for various electronic phases to be investigated.

Single-crystalline samples of K_xRhO_2 were grown by a self-flux method [36,37]. A mixture of K_2CO_3 (99.999%) and Rh_2O_3 (99.9%) with a molar ratio of 50 : 1 was put in an

*6217603@ed.tus.ac.jp
†okazaki@rs.tus.ac.jp

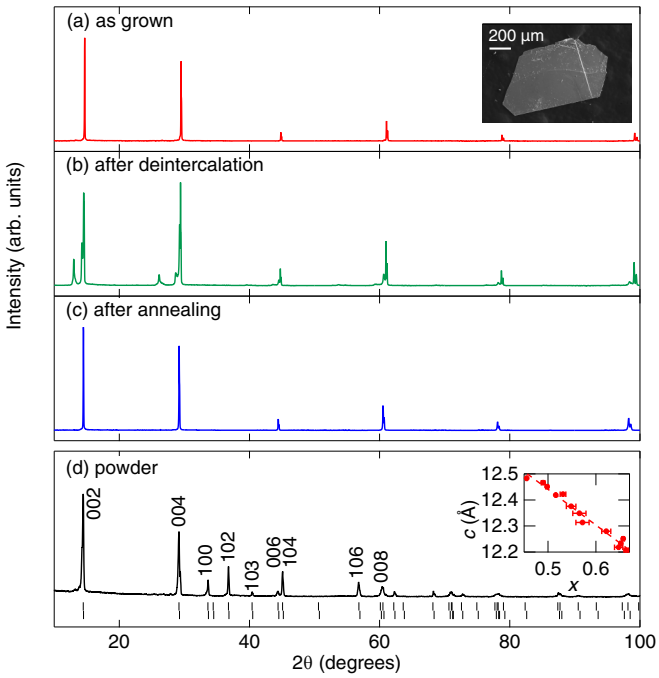

FIG. 1. (a)–(c) The XRD pattern of the single crystal: (a) as grown, (b) after deintercalation, and (c) after annealing. The inset of (a) shows the scanning electron microscopy (SEM) image of the as-grown K_xRhO_2 crystal. (d) The powder XRD pattern. Bars indicate the expected Bragg peak positions for γ-type structure K_xRhO_2. The inset shows the relation between the K content x and c-axis lattice parameter c. The dashed line represents a linear fitting result.

alumina crucible and kept at 1373 K for 1 h, and then cooled down to 1123 K with a rate of 5 K/h. After washing with distilled water, we obtained thin hexagonal crystals as shown in the inset of Fig. 1(a). X-ray diffraction (XRD) measurements were performed by an x-ray diffractometer (Rigaku Ultima IV) with Cu $K\alpha$ radiation in a θ-2θ scan mode. In the case of the single-crystalline samples, the scattering vector was normal to the surface of the sample. The K content of as-grown samples is $x \sim 0.67$. To get the lower potassium content samples, we dipped the samples in I_2-acetonitrile solutions [44]. The potassium content was controlled by both the concentration of the solution and the length of time to dip. This process was conducted at room temperature. Subsequently, we annealed these dipped samples at 473 K for about 2 days in air to obtain single-phase samples. To elucidate the relation between the c-axis lattice parameter and potassium content, we measured the K content x using an electron probe microanalyzer (JEOL JXA-8100) after we determined the c-axis lattice parameter by XRD measurement. The in-plane resistivity and the Seebeck coefficient were simultaneously measured by using a conventional dc four-probe method and a steady-state method. The thermoelectric voltage contribution from the wire leads was subtracted.

We first show the XRD patterns of a single crystal in each process of the K deintercalation. The XRD patterns of as-grown and after-deintercalation crystals are depicted in Figs. 1(a) and 1(b), respectively. As reported by Zhang *et al.* [43,44], several sets of the peaks are observed in after-deintercalation crystals. On the other hand, after annealing, we find that a single-phase pattern is recovered as shown in Fig. 1(c). In the isostructural Na_xCoO_2, it is well known that the low Na-content sample is easily hydrated and a heating process removes H_2O molecules from the hydrated sample [45]. Thus the present result indicates that a hydrated phase is also formed in K_xRhO_2 after deintercalation but can be recovered to the nonhydrated phase by successive annealing. The existence of the hydrated K_xRhO_2 is also suggested by an ion exchange experiment [46]. Note that no superconductivity is observed in the hydrated K_xRhO_2 at present.

The powder XRD pattern of the nonhydrated sample for $x = 0.651$ is represented in Fig. 1(d). Note that the measured powder is not ground and just collected as small single crystals with the size of $\sim$50 μm, because the grinding significantly induces hydration. As seen in Fig. 1(d), all the peaks are indexed using the γ-Na_xCoO_2-type structure (space group $P6_3/mmc$) with the lattice parameters of $a = 3.076(2)$ Å and $c = 12.233(5)$ Å. In earlier reports, the c-axis lattice parameter is found to be 13.6 Å [36,38], much larger than the present result. This discrepancy indicates that the powder XRD patterns in the earlier reports refer to the hydrated phase, as is also pointed out by means of the optimization of the lattice constants [41]. On the other hand, the space group is preserved among the hydrated and nonhydrated samples, similar to the case of Na_xCoO_2 [14].

We examine the relation between the c-axis lattice parameter and the K content x using nonhydrated crystals as shown in the inset of Fig. 1(d). The c-axis lattice parameter decreases almost linearly with increasing K content x. In this system, when the K content increases, the Coulomb force holding the RhO_2 layers is enhanced to decrease the c-axis lattice parameter, which is also seen in Na_xCoO_2 [2]. The present data are fitted using a linear function $c = c_0 + c_1x$ with $c_0 = 13.13(4)$ Å and $c_1 = -1.37(7)$ Å as shown by the dashed line. The K content of crystals for the transport measurements is calculated from the c-axis lattice parameter using this relation in a similar manner to that of Na_xCoO_2 [5]. The x values have a common error which is estimated at up to 0.04 due to the large error of c_0 and c_1. However, we can obtain a relative amount of K content accurately by a comparison with the c-axis lattice parameter. From the K content, the hole concentration is approximately determined as $1 - x$ holes/Rh [40].

We then discuss the transport properties of K_xRhO_2. Figure 2 shows the temperature dependence of the Seebeck coefficient and the resistivity for $x = 0.50$ and 0.51. The resistivity is normalized by the room-temperature resistivity $\rho_{RT} \sim 1$ mΩ cm, which has a large error because the sample thickness is too small to be measured correctly. We also note that the value of ρ_{RT} does not change significantly for all the crystals in the present study. A distinct anomaly is observed in both the Seebeck coefficient and resistivity at around 75 K, as marked by the dashed line. An origin of this anomaly is not clear at present. In Na_xCoO_2, the two distinct phase transitions were observed, and the ground state is a charge-ordered insulator at around $x = 0.5$ [2,5]. Moreover, an interesting topological state has been suggested theoretically for $x = 0.5$ [42].

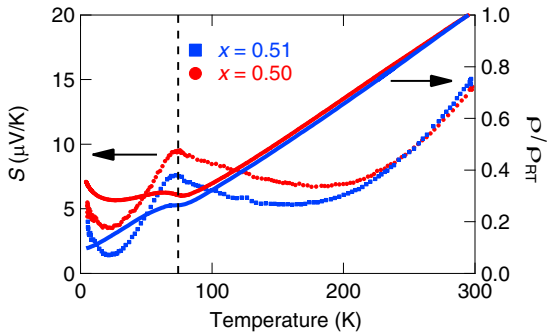

FIG. 2. Temperature dependence of the Seebeck coefficient (left axis) and the resistivity normalized by the room-temperature resistivity ρ_{RT} (right axis) of K_xRhO_2 for $x = 0.50$ and 0.51. The dashed line represents the temperature at which the distinct anomaly is observed.

We next show the temperature dependence of the transport properties for $0.57 \lesssim x \lesssim 0.67$ in Figs. 3(a) and 3(b). Around room temperature, the Seebeck coefficient almost linearly decreases with decreasing temperature for all the samples. On the other hand, the temperature dependence does not systematically vary with the K content. For $x \gtrsim 0.65$, the Seebeck coefficient is roughly proportional to temperature as shown in Fig. 3(b). In contrast, as shown in Fig. 3(a), the temperature dependence for $0.57 \lesssim x \lesssim 0.64$ is qualitatively different from that for $x \gtrsim 0.65$: At low temperatures, the Seebeck coefficient is enhanced with a broad peak structure. Note that the phonon drag effect is unlikely since we have observed a similar temperature variation even in the polycrystalline samples (not shown).

The anomaly is clearly demonstrated in the Seebeck coefficient divided by temperature, S/T, shown in Figs. 3(c) and 3(d). For $0.57 \lesssim x \lesssim 0.64$, S/T gradually increases with lowering temperature. It also increases with increasing x but the behavior drastically changes in the narrow range of

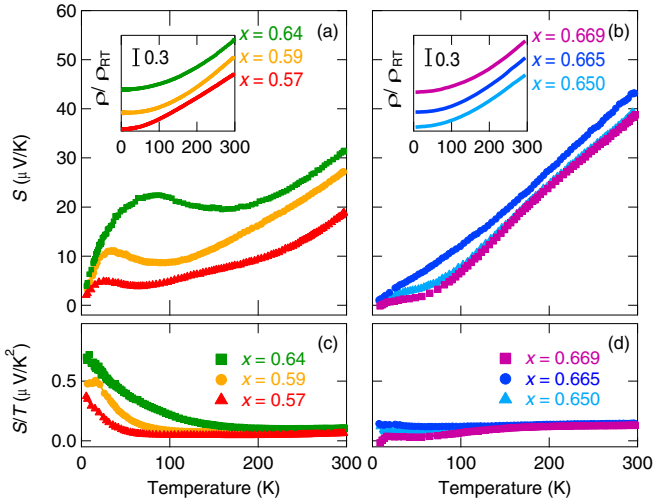

FIG. 3. The temperature dependence of (a), (b) the Seebeck coefficient and (c), (d) the Seebeck coefficient divided by temperature, S/T. The left panels show the data below $x = 0.64$ and the right panels show the data above $x = 0.65$. The insets show the normalized resistivity as a function of temperature.

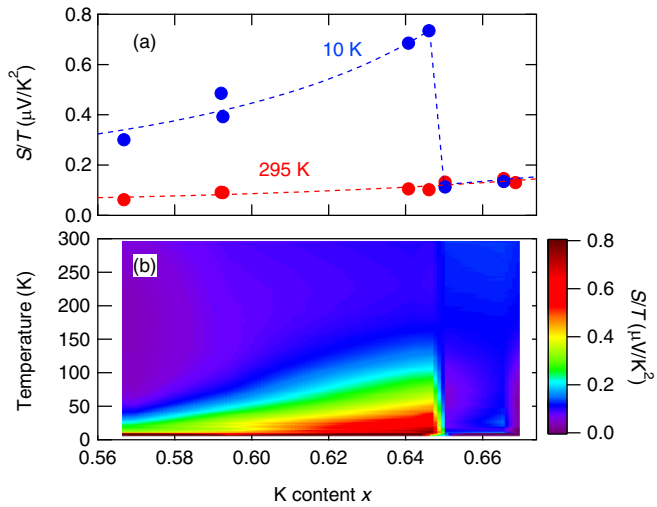

FIG. 4. (a) The x dependence of S/T of K_xRhO_2 at $T = 10$ K (blue) and 295 K (red). The dashed lines are guides for the eyes. (b) Contour plot of S/T.

$0.64 < x < 0.65$ into almost no temperature dependence, as expected in a conventional metal, suggesting that there is a critical content x^* in this narrow range. Figure 4(a) represents S/T as a function of x at constant temperatures and the contour plot is depicted in Fig. 4(b). At low temperature, S/T shows a divergent behavior at x^* only from the lower x side. This is distinct from the divergence of S/T from both sides of the critical point of the Landau-type phase transition associated with broken symmetry [47]. Also, no structural transition is observed at x^*. It is a key point that the enhancement is observed for only low temperature, while S/T continuously increases with x near room temperature, which is readily explained by the change in the carrier concentration.

Now we discuss the origin of the enhancement of the Seebeck coefficient. According to the observed band structure of $K_{0.62}RhO_2$, the Fermi level lies across the a_{1g} band [40]. The Fermi level is elevated as x increases, and as is the case in Na_xCoO_2, the topological change in the Fermi surface would also occur at a certain content in K_xRhO_2. Note that the present critical content x^* is close to $x^*_{Na} \simeq 0.62$, at which the Lifshitz transition occurs in Na_xCoO_2 [8]. Moreover, near the Lifshitz transition, the low-temperature Seebeck coefficient is predicted to increase steeply when the Fermi level approaches a critical point from only one side, the one for which the number of Fermi surfaces is larger, owing to the divergence in the energy derivative of the density of states [48,49], as is also explored in several alloys experimentally [50,51]. Thus the observed enhancement indicates the existence of a Lifshitz transition in K_xRhO_2. We also note that the resistivity has no singularity around the Lifshitz transition [49]. In the insets of Figs. 3(a) and (b), we show the temperature dependence of the normalized resistivity, which exhibits no significant change across x^*, consistent with the above picture.

We examine the detailed mechanism of the Lifshitz transition. In Fig. 5, we show the schematic band structure and the Fermi surface of Na_xCoO_2 and K_xRhO_2. Since the γ-type

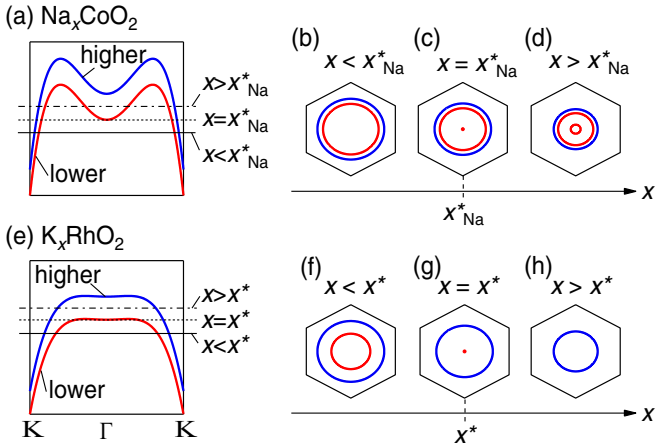

FIG. 5. Schematic pictures of (a) the band structure along the K-Γ-K line and (b)–(d) the Fermi surface as a function of the Na content x of Na_xCoO_2. (e)–(h) Corresponding band structure and the Fermi surface of K_xRhO_2. The red and blue curves represent the lower and higher bands, respectively, in common with the band structure and the Fermi surface. Near the Γ point, the band is more flat in K_xRhO_2 compared with that of Na_xCoO_2. As x increases, the electron pocket suddenly appears at $x = x^*_{Na}$ in Na_xCoO_2 while the inner hole cylinder gradually diminishes and then disappears at $x = x^*$ in K_xRhO_2.

structure has two Co/Rh ions in the unit cell, we consider two a_{1g} bands labeled as higher and lower bands in Figs. 5(a) and 5(e) [19], although these are almost degenerate and difficult to be resolved separately by ARPES measurements. In Na_xCoO_2, there are two hole cylinders for $x < x^*_{Na}$ as shown in Fig. 5(b), and with increasing x, the Fermi level rises and then touches the local minimum of the lower band at $x = x^*_{Na}$ [Fig. 5(c)] to create a small electron pocket at the Γ point for $x > x^*_{Na}$ [Fig. 5(d)]. In this case, the low-temperature Seebeck coefficient would be critically enhanced owing to the disappearance of the electron pocket only when x approaches x^*_{Na} from the high x side. Indeed, a negatively enhanced Seebeck coefficient is seen for $x > x^*_{Na}$, although the experiments have been done in polycrystalline samples [8].

On the other hand, the enhancement of the Seebeck coefficient is observed for $x < x^*$ in K_xRhO_2, indicating that the topological change in the Fermi surfaces differs from that of Na_xCoO_2. According to a recent ARPES measurement [40], the band structure of K_xRhO_2 is closely similar to that of Na_xCoO_2, and thus we consider a local minimum structure at the Γ point as well. In Na_xCoO_2, this minimum structure is induced by a third nearest hopping t_3, and the local minimum sinks more deeply as the ratio $|t_3/t_1|$ becomes larger (t_1 being the first nearest hopping) [28]. Now, the $4d$ orbital is broader than the $3d$ one, but the ionic radius of Rh is also larger than Co, resulting in an accidental cancellation of the effect of the broader $4d$ orbital in some materials [52]. In K_xRhO_2, the broader bandwidth is indeed observed [39,40], but $|t_3/t_1|$ may be smaller than that of Na_xCoO_2 because the oxygen $2p$ contribution in t_3 would be small due to the larger Rh-Rh distance. In such a case, the local minimum structure of the band top would be shallow in K_xRhO_2 as illustrated in Fig. 5(e), also implied by the density functional theory (DFT) calculations [40].

This scenario is schematically depicted in Figs. 5(e)–5(h). In K_xRhO_2, the shallow local minimum structure may be undetectable because of thermal fluctuations even at low temperatures. For increasing x, the Fermi level is elevated and then the lower a_{1g} band is fully occupied at x^*. In this case, the inner hole cylinder gradually diminishes and then completely disappears for $x > x^*$, which is also supported by a highly 2D character of the Fermi surface [40]. Thus, in K_xRhO_2, the low-temperature enhancement of S/T occurs only for $x < x^*$, where the number of hole cylinders is larger than that for $x > x^*$. It should be noted that the disappearance of the electron pocket in Na_xCoO_2 contributes to the Seebeck coefficient negatively but the disappearance of the hole cylinder in K_xRhO_2 contributes positively, enhancing the total Seebeck coefficient that also includes the contribution from the outer hole cylinder. Therefore, our results suggest the Lifshitz transition as a fundamental means to increase the Seebeck coefficient at low temperatures in this system, in addition to the previously reported pudding-mold band structure [28] and the large entropy flow of the d electrons [53].

To summarize, we have synthesized single-crystal K_xRhO_2 for $0.50 \lesssim x \lesssim 0.67$ and find that, while the Seebeck coefficient monotonically increases with increasing x near room temperature, it exhibits an enhancement at low temperatures only below $x^* \simeq 0.65$. As an origin, we propose a Lifshitz transition associated with the disappearance of the inner hole cylinder due to the flat band structure around the Γ point. Moreover, we have discovered a distinct phase transition for $x \sim 0.5$, suggesting that K_xRhO_2 also offers a fascinating platform for various electronic phases, similar to Na_xCoO_2.

We thank K. Fujimoto, H. Yaguchi, and T. Yamanaka for discussions, and D. Kabasawa and W. Takagi for experimental support. This work was supported by JSPS KAKENHI Grants No. JP17H06136, No. JP18K03503, and No. JP18K13504.

[1] I. Terasaki, Y. Sasago, and K. Uchinokura, Phys. Rev. B **56**, R12685(R) (1997).
[2] M. L. Foo, Y. Wang, S. Watauchi, H. W. Zandbergen, T. He, R. J. Cava, and N. P. Ong, Phys. Rev. Lett. **92**, 247001 (2004).
[3] T. Motohashi, E. Naujalis, R. Ueda, K. Isawa, M. Karppinen, and H. Yamauchi, Appl. Phys. Lett. **79**, 1480 (2001).
[4] M. Lee, L. Viciu, L. Li, Y. Wang, M. L. Foo, S. Watauchi, R. A. Pascal, R. J. Cava, and N. P. Ong, Nat. Mater. **5**, 537 (2006).
[5] M. Yokoi, T. Moyoshi, Y. Kobayashi, M. Soda, Y. Yasui, M. Sato, and K. Kakurai, J. Phys. Soc. Jpn. **74**, 3046 (2005).
[6] D. Yoshizumi, Y. Muraoka, Y. Okamoto, Y. Kiuchi, J. Yamaura, M. Mochizuki, M. Ogata, and Z. Hiroi, J. Phys. Soc. Jpn. **76**, 063705 (2007).

[7] G. Lang, J. Bobroff, H. Alloul, G. Collin, and N. Blanchard, Phys. Rev. B **78**, 155116 (2008).

[8] Y. Okamoto, A. Nishio, and Z. Hiroi, Phys. Rev. B **81**, 121102(R) (2010).

[9] T. Motohashi, R. Ueda, E. Naujalis, T. Tojo, I. Terasaki, T. Atake, M. Karppinen, and H. Yamauchi, Phys. Rev. B **67**, 064406 (2003).

[10] B. C. Sales, R. Jin, K. A. Affholter, P. Khalifah, G. M. Veith, and D. Mandrus, Phys. Rev. B **70**, 174419 (2004).

[11] Q. Huang, M. L. Foo, J. W. Lynn, H. W. Zandbergen, G. Lawes, Y. Wang, B. H. Toby, A. P. Ramirez, N. P. Ong, and R. J. Cava, J. Phys.: Condens. Matter **16**, 5803 (2004).

[12] J. Sugiyama, J. H. Brewer, E. J. Ansaldo, H. Itahara, T. Tani, M. Mikami, Y. Mori, T. Sasaki, S. Hébert, and A. Maignan, Phys. Rev. Lett. **92**, 017602 (2004).

[13] F. L. Ning, S. M. Golin, K. Ahilan, T. Imai, G. J. Shu, and F. C. Chou, Phys. Rev. Lett. **100**, 086405 (2008).

[14] K. Takada, H. Sakurai, E. Takayama-Muromachi, F. Izumi, R. A. Dilanian, and T. Sasaki, Nature (London) **422**, 53 (2003).

[15] R. Jin, B. C. Sales, P. Khalifah, and D. Mandrus, Phys. Rev. Lett. **91**, 217001 (2003).

[16] I. I. Mazin and M. D. Johannes, Nat. Phys. **1**, 91 (2005).

[17] H. D. Yang, J.-Y. Lin, C. P. Sun, Y. C. Kang, C. L. Huang, K. Takada, T. Sasaki, H. Sakurai, and E. Takayama-Muromachi, Phys. Rev. B **71**, 020504(R) (2005).

[18] M. Ogata, J. Phys.: Condens. Matter **19**, 145282 (2007).

[19] D. J. Singh, Phys. Rev. B **61**, 13397 (2000).

[20] M. M. Korshunov, I. Eremin, A. Shorikov, V. I. Anisimov, M. Renner, and W. Brenig, Phys. Rev. B **75**, 094511 (2007).

[21] K. Kuroki, S. Ohkubo, T. Nojima, R. Arita, S. Onari, and Y. Tanaka, Phys. Rev. Lett. **98**, 136401 (2007).

[22] M. Z. Hasan, Y.-D. Chuang, D. Qian, Y. W. Li, Y. Kong, A. Kuprin, A. V. Fedorov, R. Kimmerling, E. Rotenberg, K. Rossnagel, Z. Hussain, H. Koh, N. S. Rogado, M. L. Foo, and R. J. Cava, Phys. Rev. Lett. **92**, 246402 (2004).

[23] H.-B. Yang, S.-C. Wang, A. K. P. Sekharan, H. Matsui, S. Souma, T. Sato, T. Takahashi, T. Takeuchi, J. C. Campuzano, R. Jin, B. C. Sales, D. Mandrus, Z. Wang, and H. Ding, Phys. Rev. Lett. **92**, 246403 (2004).

[24] H.-B. Yang, Z.-H. Pan, A. K. P. Sekharan, T. Sato, S. Souma, T. Takahashi, R. Jin, B. C. Sales, D. Mandrus, A. V. Fedorov, Z. Wang, and H. Ding, Phys. Rev. Lett. **95**, 146401 (2005).

[25] D. Qian, L. Wray, D. Hsieh, D. Wu, J. L. Luo, N. L. Wang, A. Kuprin, A. Fedorov, R. J. Cava, L. Viciu, and M. Z. Hasan, Phys. Rev. Lett. **96**, 046407 (2006).

[26] J. Geck, S. V. Borisenko, H. Berger, H. Eschrig, J. Fink, M. Knupfer, K. Koepernik, A. Koitzsch, A. A. Kordyuk, V. B. Zabolotnyy, and B. Büchner, Phys. Rev. Lett. **99**, 046403 (2007).

[27] T. Arakane, T. Sato, T. Takahashi, T. Fujii, and A. Asamitsu, New J. Phys. **13**, 043021 (2011).

[28] K. Kuroki and R. Arita, J. Phys. Soc. Jpn. **76**, 083707 (2007).

[29] I. M. Lifshitz, Sov. Phys. JETP **11**, 1130 (1960).

[30] H. Watanabe, Y. Mori, M. Yokoi, T. Moyoshi, and M. Soda, J. Phys. Soc. Jpn. **75**, 034716 (2006).

[31] M. Yokoi, Y. Kobayashi, T. Moyoshi, and M. Sato, J. Phys. Soc. Jpn. **77**, 074704 (2008).

[32] K.-W. Lee and W. E. Pickett, Phys. Rev. B **76**, 134510 (2007).

[33] A. Varela, M. Parras, and J. M. González-Calbet, Eur. J. Inorg. Chem. **2005**, 4410 (2005).

[34] Y. Krockenberger, M. Reehuis, G. Cristiani, C. Ritter, H.-U. Habermeier, and L. Alff, Physica C **460–462**, 468 (2007).

[35] B.-B. Zhang, C. Wang, S.-T. Dong, Y.-Y. Lv, L. Zhang, Y. Xu, Y. B. Chen, J. Zhou, S.-H. Yao, and Y.-F. Chen, Inorg. Chem. **57**, 2730 (2018).

[36] K. Yubuta, S. Shibasaki, I. Terasaki, and T. Kajitani, Philos. Mag. **89**, 2813 (2009).

[37] S. Shibasaki, T. Nakano, I. Terasaki, and T. Kajitani, J. Phys.: Condens. Matter **22**, 115603 (2010).

[38] S. H. Yao, B. B. Zhang, J. Zhou, Y. B. Chen, S. T. Zhang, Z. B. Gu, S. T. Dong, and Y. F. Chen, AIP Adv. **2**, 042140 (2012).

[39] R. Okazaki, Y. Nishina, Y. Yasui, S. Shibasaki, and I. Terasaki, Phys. Rev. B **84**, 075110 (2011).

[40] S.-D. Chen, Y. He, A. Zong, Y. Zhang, M. Hashimoto, B.-B. Zhang, S.-H. Yao, Y.-B. Chen, J. Zhou, Y.-F. Chen, S.-K. Mo, Z. Hussain, D. Lu, and Z.-X. Shen, Phys. Rev. B **96**, 081109(R) (2017).

[41] Y. Saeed, N. Singh, and U. Schwingenschlögl, Adv. Funct. Mater. **22**, 2792 (2012).

[42] J. Zhou, Q.-F. Liang, H. Weng, Y. B. Chen, S.-H. Yao, Y.-F. Chen, J. Dong, and G.-Y. Guo, Phys. Rev. Lett. **116**, 256601 (2016).

[43] B.-B. Zhang, S.-T. Dong, Y. B. Chen, L.-Y. Zhang, J. Zhou, S. H. Yao, Z.-B. Gu, S.-T. Zhang, and Y.-F. Chen, CrystEngComm **15**, 5050 (2013).

[44] B.-B. Zhang, Y.-Y. Lv, S.-T. Dong, L.-Y. Zhang, S.-H. Yao, Y. B. Chen, S.-T. Zhang, J. Zhou, and Y.-F. Chen, Solid State Commun. **230**, 1 (2016).

[45] D. P. Chen, H. C. Chen, A. Maljuk, A. Kulakov, H. Zhang, P. Lemmens, and C. T. Lin, Phys. Rev. B **70**, 024506 (2004).

[46] A. Mendiboure, H. Eickenbusch, and R. Schöllhorn, J. Solid State Chem. **71**, 19 (1987).

[47] H. Sakai, K. Ikeura, M. S. Bahramy, N. Ogawa, D. Hashizume, J. Fujioka, Y. Tokura, and S. Ishiwata, Sci. Adv. **2**, e1601378 (2016).

[48] A. A. Abrikosov, *Fundamentals of the Theory of Metals* (Dover, New York, 1988).

[49] A. A. Varlamov, V. S. Egorov, and A. V. Pantsulaya, Adv. Phys. **38**, 469 (1989).

[50] V. S. Egorov and A. N. Fedorov, JETP Lett. **35**, 462 (1982).

[51] V. S. Egorov, M. Yu Lavrenyuk, N. Ya. Minina, and A. M. Savin, JETP Lett. **40**, 750 (1984).

[52] S. Okada, I. Terasaki, H. Okabe, and M. Matoba, J. Phys. Soc. Jpn. **74**, 1525 (2005).

[53] W. Koshibae, K. Tsutsui, and S. Maekawa, Phys. Rev. B **62**, 6869 (2000).